

Exclusive measurement of coherent η photoproduction from the deuteron

J. Weiß¹, P. Achenbach², J. Ahrens², J.R.M. Annand³, R. Beck², V. Hejny⁴, J.D. Kellie³, V. Kleber⁴, M. Kotulla¹, B. Krusche⁵, V. Kuhr⁶, R. Leukel², V. Metag¹, V. M. Olmos de León², F. Rambo⁶, A. Schmidt², U. Siodlaczek⁷, H. Ströher⁴, F. Wissmann⁶, and M. Wolf¹

¹ II. Physikalisches Institut, Justus-Liebig-Universität Gießen, Heinrich-Buff-Ring 16, D-35392 Gießen

² Institut für Kernphysik, Johannes-Gutenberg-Universität Mainz, Johannes-Joachim-Becher-Weg 45, D-55099 Mainz

³ Department of Physics and Astronomy, University of Glasgow, Glasgow G128QQ, UK

⁴ Institut für Kernphysik, Forschungszentrum Jülich GmbH, D-52425 Jülich

⁵ Departement für Physik und Astronomie, Universität Basel, Klingelbergstrasse 82, CH-4056 Basel

⁶ II. Physikalisches Institut, Georg-August-Universität Göttingen, Bunsenstr. 7-9, D-37073 Göttingen

⁷ Physikalisches Institut, Eberhard-Karls-Universität Tübingen, Auf der Morgenstelle 14, D-72076 Tübingen

May 5, 2019

Abstract. Coherent photoproduction of η mesons from the deuteron has been measured from threshold up to $E_\gamma \approx 750$ MeV using the photon spectrometer TAPS at the tagged photon facility at the Mainz microtron MAMI. For the first time, differential coherent cross sections have been deduced from the coincident detection of the η meson and the recoil deuteron. A missing energy analysis was used for the suppression of background events so that a very clean identification of coherent η -photoproduction was achieved. The resulting cross sections agree with previous experimental results except for angles around 90° in the γd cm system where they are smaller. They are compared to various model calculations.

PACS. 13.60.Le meson production – 14.20.Gk baryon resonances with S=0 – 25.20.Lj photoproduction reactions

1 Introduction

The structure of the nucleon and its excited states is one of the central issues of nonperturbative Quantum Chromodynamics. Meson photoproduction has emerged as an excellent tool for experimental investigations providing detailed resonance properties which are the ideal testing ground for modern hadron models. One of the major difficulties for the experimental study of excited nucleon states is that they are closely spaced and, due to their hadronic decay channels, have large widths which result in a significant overlap. Furthermore non-resonant background contributions like nucleon Born terms or vector meson exchange complicate the interpretation of photoproduction reactions. However, there are a few cases where, due to the different couplings of the resonances to the initial photon - nucleon state and the final nucleon - meson states, certain resonances strongly dominate photoproduction reactions. The best known example is the dominance of the low lying $P_{33}(1232)$ Δ -resonance in π^0 -photoproduction. In the so-called second resonance region which comprises the $P_{11}(1440)$, $D_{13}(1520)$ and $S_{11}(1535)$ resonances the largest contribution to pion photoproduction comes from

the excitation of the D_{13} due to the large photon coupling. On the other hand η -photoproduction in this energy range proceeds almost exclusively via the excitation of the S_{11} resonance [1, 2]. The decay branching ratio of this resonance into $N\eta$ is approximately 50% [3] while for the D_{13} it is less than 1% [4]. Eta photoproduction is therefore the best reaction for the study of the S_{11} resonance on the free nucleon [1] and in nuclear matter [5, 6]. The negligible contribution of the P_{11} - and D_{13} -resonances to η -photoproduction is easily understood since these decays must proceed via η - nucleon pairs with relative orbital angular momenta of $l = 1, 2$ which are strongly suppressed close to threshold. However, it is not understood why the contribution of the $S_{11}(1650)$ is also very small.

Eta photoproduction from the proton has been used to determine the basic properties of the $S_{11}(1535)$ resonance, such as its mass, width and in particular the electromagnetic helicity amplitude $A_{1/2}^p$ [1, 2]. The isospin structure of the electromagnetic excitation of the $S_{11}(1535)$ resonance was investigated in experiments on η photoproduction from the deuteron [7, 8]. Quasifree η -photoproduction from the deuteron can be used to deduce the cross section of the $n(\gamma, \eta)n$ reaction. However the complete isospin decomposition requires in addition the measurement of coherent photoproduction from an isospin $I=0$ nucleus. Since

the excitation of the S_{11} -resonance via the E_{0+} multipole involves a spin-flip transition, the $I=0, J=1$ deuteron is the ideal target nucleus for this purpose. The isospin composition can be deduced from these measurements via:

$$\sigma_p \sim |A_{1/2}^s + A_{1/2}^v|^2 = |A_{1/2}^p|^2 \quad (1)$$

$$\sigma_n \sim |A_{1/2}^s - A_{1/2}^v|^2 = |A_{1/2}^n|^2 \quad (2)$$

$$\sigma_d^{\text{coh}} \sim |A_{1/2}^s|^2 \quad (3)$$

where $A_{1/2}^s$ denotes the isoscalar and $A_{1/2}^v$ the isovector amplitude.

While quark models and results from pion photoproduction predicted a dominant isovector component of the $S_{11}(1535)$ excitation, an early experiment found a large coherent eta production cross section from the deuteron [9], requiring a large isoscalar contribution. More recent experiments found the cross section to be much lower [7,8] and extracted $A_{1/2}^s < A_{1/2}^v$, as quark models have predicted. Furthermore, from inclusive and exclusive measurements of quasi-free η photoproduction from the deuteron and ${}^4\text{He}$, a cross section ratio of $|A_{1/2}^n|^2/|A_{1/2}^p|^2 = \sigma_n/\sigma_p \approx 0.66$ has been deduced [7,8,10]. Taking into account the small coherent cross section from the deuteron a ratio of $|A_{1/2}^s|/|A_{1/2}^p| = 0.09$ was extracted in [7,8].

On the other hand models reproducing the measured cross section of coherent η photoproduction from the deuteron [11,12] require $|A_{1/2}^s|/|A_{1/2}^p| = 0.22 - 0.26$, a value in conflict with the experimental result above (cf. sec. 3). This discrepancy motivated further studies of coherent photoproduction of η mesons from the deuteron. Ritz et al. [13] recently suggested that the problem is due to contributions from hadronic rescattering which give rise to a complex, energy-dependent phase relation between the extracted amplitudes. They deduce from a fit of their model to the data $A_{1/2}^p = (120.0 - i66.1) \times 10^{-3} \text{GeV}^{-1/2}$, $A_{1/2}^n = (-114.0 - i1.7) \times 10^{-3} \text{GeV}^{-1/2}$ which are consistent with $|A_{1/2}^n|^2/|A_{1/2}^p|^2 \approx 0.66$ and $|A_{1/2}^s|/|A_{1/2}^p| \approx 0.25$.

2 Experimental setup and analysis methods

Coherent photoproduction of η mesons has been measured at the Glasgow tagged photon facility [14] at the Mainz microtron MAMI [15,16] using the photon spectrometer TAPS. A quasi-monochromatic photon beam of energies up to 818 MeV was produced via bremsstrahlung tagging. The TAPS detector [17,18] consisted of 6 blocks each with 64 hexagonal cross section BaF_2 crystals and a forward detector with 120 BaF_2 crystals. The 6 blocks were located in a horizontal plane around the target at angles of $\pm 50^\circ$, $\pm 100^\circ$, and $\pm 150^\circ$ with respect to the beam axis. The forward detector covered a polar angular range of $5^\circ < \theta < 20^\circ$. This setup subtended $\approx 30\%$ of the full solid angle. All BaF_2 modules were equipped with 5 mm thick plastic detectors for the identification of charged particles. The target was a 10 cm long, 4 cm diameter, liquid deuterium

filled cell. A detailed description of the setup is given in [10].

Eta mesons were detected via their two photon decay channel and identified in a standard invariant mass analysis using the measured photon energies and angles as input. An invariant mass resolution of ≈ 60 MeV (FWHM) was achieved for the η signal. The photons were identified by time of flight and pulse shape analysis, while deuteron identification relied on energy and energy loss information from the plastic and BaF_2 scintillators (see [10] for details). A missing energy analysis which utilises the kinematical overdetermination of the reaction was performed to obtain clear identification of coherent events. The difference of the c.m. energies of both the η (E_η^*) and the deuteron (E_d^*) was calculated for this purpose from initial and final state kinematic quantities as follows:

$$E_{\text{miss}}^d = E_d^*(E_\gamma, m_d) - E_d^*(E_d^{\text{lab}}, \mathbf{p}_d^{\text{lab}}) \quad (4)$$

$$E_{\text{miss}}^\eta = E_\eta^*(E_\gamma, m_d) - E_\eta^*(E_\eta^{\text{lab}}, \mathbf{p}_\eta^{\text{lab}}) \quad (5)$$

where E_γ denotes the incident photon beam energy, m_d the deuteron mass, $E_{d,\eta}^{\text{lab}}$ and $\mathbf{p}_{d,\eta}^{\text{lab}}$ the measured energies and momenta of deuteron and η meson. The resulting two-dimensional missing energy distribution (see fig. 1) allows a very efficient discrimination of the signal from remaining background. The peak at zero (marked with an arrow), which is clearly separated from the background, corresponds to the coherent events.

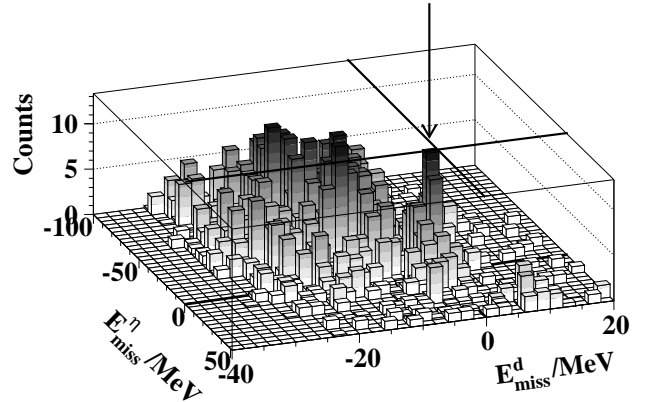


Fig. 1. Missing energy of both detected particles calculated according to eq. 4 and 5. The peak corresponding to coherent events is marked with an arrow.

The acceptance of TAPS for η -meson decays into two photons in the energy range of interest covers the full polar angle of the η -mesons. However, for the deuteron there are regions, where the particle escapes detection. Fig. 2 shows the acceptance of TAPS for coherent events as a function of photon beam energy and η polar angle in the c.m. system. The boundaries are determined by the angular range covered by the forward detector ($5^\circ < \theta < 20^\circ$) and the

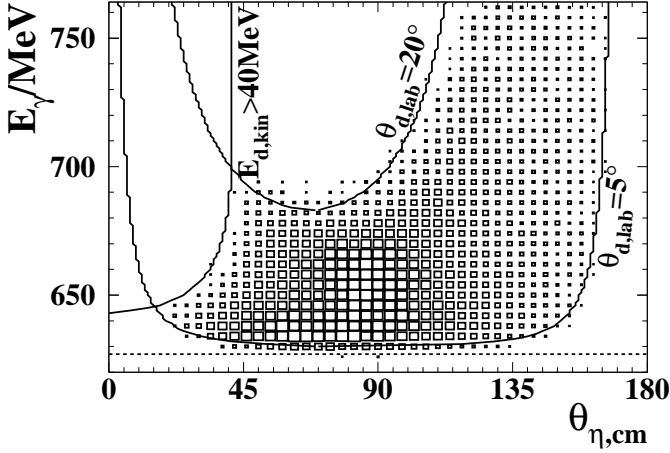


Fig. 2. Simulated acceptance for coherent η -production in TAPS. The boundaries correspond to the borders of the forward detector and the minimum energy required for the deuteron to be detected. The efficiency ranges from 1.5 to 2.8%.

minimum kinetic energy required for the detection of the deuterons ($E_{kin} > 40\text{MeV}$).

3 Results

The measured differential cross sections for coherent η photoproduction from the deuteron are summarized in figs. 3 and 4. The results of measurements performed at ELSA [8] with the AMADEUS and PHOENICS detectors are shown for comparison. The identification of coherent η -production in all previous experiments relied completely on a missing mass analysis of the detected deuterons. The η -mesons were not identified via their invariant mass which increased counting statistics through the inclusion of the $\eta \rightarrow 3\pi$ decay channels. By contrast, the TAPS experiment detected deuterons *and* η -mesons in coincidence. This improves substantially the suppression of background, in particular from double π^0 production.

The resulting differential cross section for the backward angle bins shows a rise at production threshold, falling off again above 675 MeV photon energy. The comparison of the differential cross sections around $\theta_\eta^* = 90^\circ$ measured by the different experiments shows, that the TAPS result is about 50% lower than that of PHOENIX (fig. 3). However, both results could be consistent within the statistical uncertainties. The difference to the AMADEUS data near threshold is much larger. The lowest part of fig. 3 shows the angular range of $0.62 < \cos\theta_\eta^* < 0.93$, which is not covered by the TAPS acceptance. Fix and Arenhövel [11] have compared their calculations with the PHOENICS data in this angular region. Using $|A_s|/|A_s + A_v| = 0.09$ (cf. sec. 1), the magnitude of the measured cross section is not reproduced. Instead a ratio of 0.26 is needed to fit the data. In the region around $\theta_\eta^* = 90^\circ$, the model describes the TAPS data only with the same large value of the amplitude ratio. The

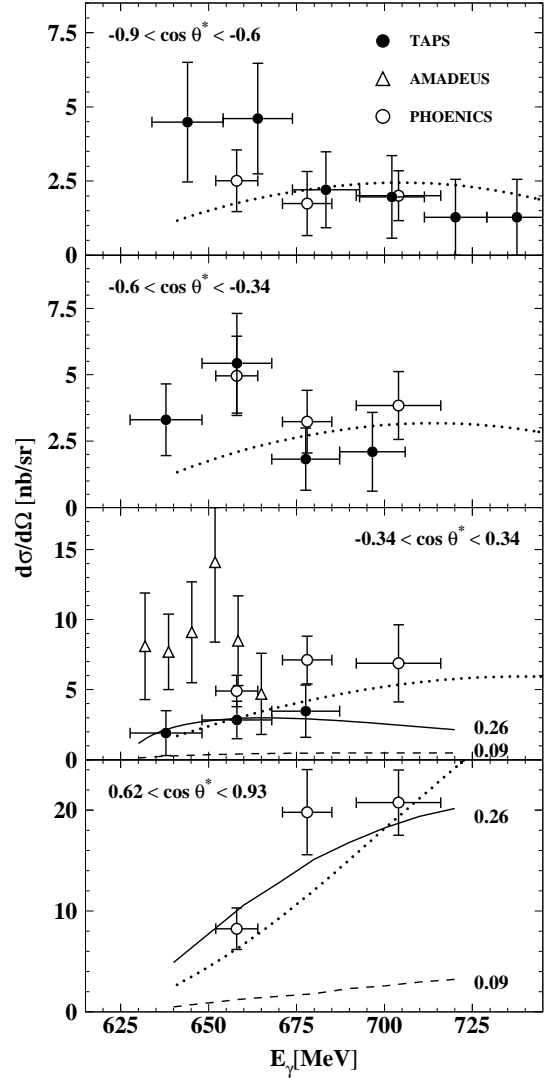


Fig. 3. Excitation function for coherent photoproduction from the deuteron measured with TAPS (● The horizontal error bars indicate the width of the incident photon energy bins) for different angular regions in comparison with experimental data from PHOENICS (○) and AMADEUS (△) [8]. The PHOENICS data for backward angles correspond to slightly different angular bins than the TAPS data (-1,-06; -0.6,-0.2). The lowest plot shows the forward region, where TAPS has no acceptance. Calculations of Fix and Arenhövel [11] for various values of $|A_{1/2}^s|/|A_{1/2}^p|$ (solid: 0.26, dashed: 0.09) and Ritz and Arenhövel [13] (dotted) are compared to the data.

calculation of Ritz et al. [13] agrees with the TAPS and PHOENICS data quite reasonably except for the lowest incident photon energies at backward angles.

The situation is similar for the η angular distributions. Fig. 4 shows the coherent η angular distributions in the photon deuteron c.m. system for different ranges of the incident photon energy. The data are compared to a calculation of Kamalov et al. [12]. This model uses the coupled channel method in plane wave (PWIA) and distorted wave (DWIA) impulse approximations. The model predictions

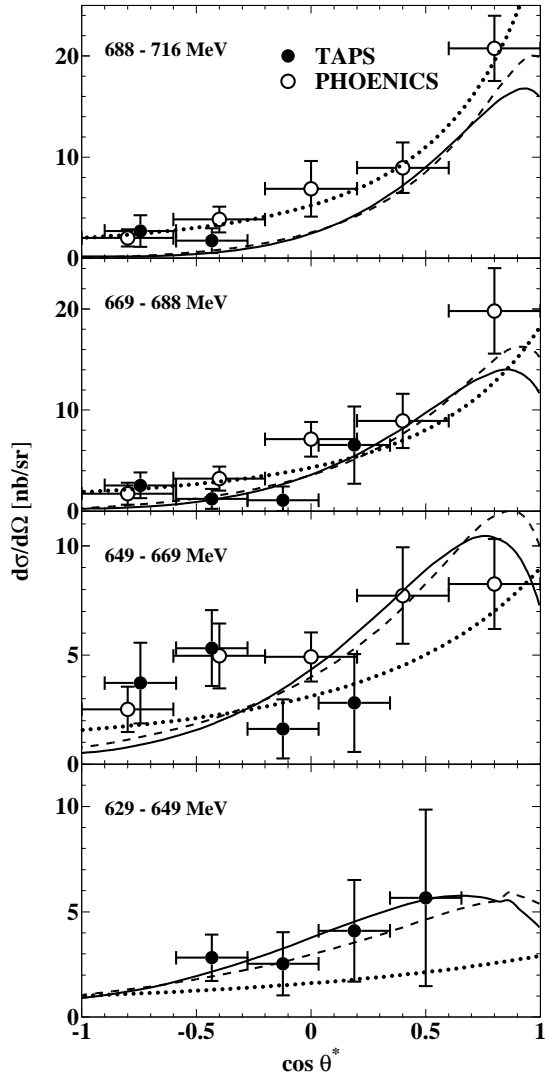


Fig. 4. Angular distributions of coherent η mesons produced from the deuteron for different photon beam energy regions (● TAPS, ○ PHOENIX, horizontal error bars represent the angular bin width). Calculations are PWIA (dashed) and DWIA (solid) from Kamalov et al. [12] for $|A_{1/2}^s|/|A_{1/2}^p| = 0.22$ and from Ritz et al. [13] (dotted).

agree with the data within the statistical uncertainty assuming $|A_s|/|A_s + A_v| = 0.22$. With the exception of the lowest incident photon energy the calculation of Ritz et al. [13] is in similar agreement with the data.

4 Conclusion

Coherent η photoproduction from the deuteron has been measured by coincident registration of the recoil deuteron *and* the η meson which very efficiently suppresses possible background contributions. The cross sections agree for most kinematical regimes with the results from a previous experiment [8] but they are smaller in the angular range around 90° in particular when compared to the AMADEUS data. Calculations in the framework of

different models are in reasonable agreement with the data when the contribution of the isoscalar amplitude is chosen in the range $|A_{1/2}^s|/|A_{1/2}^s + A_{1/2}^v| \approx 0.22 - 0.25$. This relatively large isoscalar contribution can be reconciled with the measured proton/neutron cross section ratio $|A_{1/2}^n|^2/|A_{1/2}^p|^2 = \sigma_n/\sigma_p \approx 0.66$ if rescattering contributions give rise to a large relative phase between the proton and neutron amplitudes [13]. However, the interpretation of the $d(\gamma, \eta)d$ reaction involves the isospin composition of the S_{11} excitation and at the same time the correct treatment of nuclear effects such as meson rescattering contributions. The best way to disentangle these aspects is the investigation of the coherent process for nuclei with different quantum numbers which act as spin/isospin filters. Particularly interesting is a comparison of the $I=0, J=1$ deuteron to the $I=J=1/2$ nucleus ^3He . In the latter case, as in the process on the free nucleon, the reaction is dominated by the large isovector, spin-flip amplitude. Consequently, relatively large cross sections are expected and the reaction is ideally suited to test the model treatment of the FSI effects. This reaction has been measured in a very recent experiment with TAPS at MAMI and the data are currently under analysis.

5 Acknowledgements

The authors gratefully acknowledge the outstanding support of the accelerator group of the Mainz microtron MAMI, as well as the other technicians and scientists of the Institut für Kernphysik at the Universität Mainz. We would like to thank H. Arenhövel, A. Fix, S. Kamalov and F. Ritz for discussions and correspondence.

This work was supported by Deutsche Forschungsgemeinschaft (SFB 201) and the U.K. Engineering and Physical Sciences Research Council.

References

1. B. Krusche et al., Phys. Rev. Lett. **74** (1995) 3736
2. B. Krusche et al., Phys. Lett. **B397** (1997) 171
3. C. Caso et al., Eur. Phys. J. **C3** (1998) 1
4. L. Tiator et al., Phys. Rev. **C60** (1999) 35210
5. M. Rößig-Landau et al., Phys. Lett. **B373** (1996) 45
6. T. Yorita et al., Phys. Lett. **B476** (2000) 226
7. B. Krusche et al., Phys. Lett. **B358** (1995) 40
8. P. Hoffmann-Rothe et al., Phys. Rev. Lett. **78** (1997) 4697
9. R. L. Anderson and R. Prepost, Phys. Rev. Lett. **23** (1969) 46
10. V. Hejny et al., Eur. Phys. J. **A6** (2000) 83
11. A. Fix and H. Arenhövel, Z. Phys. **A359** (1997) 427
12. S.S. Kamalov, L. Tiator, and C. Bennhold, Phys. Rev. **C55** (1997) 98
13. F. Ritz and H. Arenhövel, Phys. Rev. C, accepted (nucl-th/0011089)
14. I. Anthony et al., Nucl. Instr. Meth. **A301** (1991) 230
15. Th. Walcher, Prog. Part. Nucl. Phys. **24** (1990) 189
16. J. Ahrens et al., Nuclear Physics News **4** (1994) 5
17. R. Novotny, IEEE Trans. Nucl. Sci. **38** (1991) 379
18. A.R. Gabler et al., Nucl. Inst. and Meth. **A346** (1994) 168